AIP | The Journal of Chemical Physics

Membrane formation by preferential solvation of ions in mixture of water, 3-methylpyridine, and sodium tetraphenylborate

Koichiro Sadakane, Michihiro Nagao, Hitoshi Endo, and Hideki Seto

Citation: The Journal of Chemical Physics **139**, 234905 (2013); doi: 10.1063/1.4838795
View online: http://dx.doi.org/10.1063/1.4838795
View Table of Contents: http://scitation.aip.org/content/aip/journal/jcp/139/23?ver=pdfcov
Published by the AIP Publishing

Membrane formation by preferential solvation of ions in mixture of water, 3-methylpyridine, and sodium tetraphenylborate

Koichiro Sadakane,[1,a)] Michihiro Nagao,[2,3] Hitoshi Endo,[4] and Hideki Seto[4]
[1]*Department of Physics, Ritsumeikan University, Noji-Higashi 1-1-1, Kusatsu 525-8577, Japan*
[2]*NIST Center for Neutron Research, National Institute of Standards and Technology, Gaithersburg, Maryland 20899-6102, USA*
[3]*Center for Exploration of Energy and Matter, Indiana University, Bloomington, Indiana 47408-1398, USA*
[4]*KENS and CMRC, Institute of Materials Structure Science, High Energy Accelerator Research Organization, Tsukuba 305-0801, Japan*

(Received 4 June 2013; accepted 19 November 2013; published online 19 December 2013)

The structure and dynamics of a ternary system composed of deuterium oxide (D_2O), 3-methylpyridine (3MP), and sodium tetraphenylborate ($NaBPh_4$) are investigated by means of small-angle neutron scattering (SANS) and neutron spin echo (NSE) techniques. In the SANS experiments, a structural phase transition is confirmed between a disordered-phase and an ordered-lamellar-phase upon variation of the composition and/or temperature of the mixture. The characteristic lengths of the structures is on the sub-micrometer scale. A dispersion relation of the structure is measured through NSE experiments, which shows that the relaxation rate follows a cubic relation with momentum transfer. This implies that the dynamics of the system are determined predominantly by membrane fluctuations. The present results indicate that 3MP-rich domains are microscopically separated from bulk water in the presence of $NaBPh_4$, and that the layers behave as membranes. These results are interpreted that preferential solvation of salt in each solvent induces a microphase separation between the solvents, and the periodic structure of 3MP-rich domains is stabilized by the long-range electrostatic interaction arising from Na^+ ions in D_2O-rich domains. © *2013 AIP Publishing LLC*. [http://dx.doi.org/10.1063/1.4838795]

I. INTRODUCTION

Binary mixtures of water and organic solvents have been investigated for the study of phase separation and associated critical phenomena.[1] From experiments, it is known that the two-phase region of a binary mixture expands when a hydrophilic salt such as NaCl or NaBr is added.[2–5] It is well known that the interfacial energy between water and an organic solvent increases with the addition of a hydrophilic salt,[6] and this could be a factor in salt-induced phase separation. Thus, the effect of a hydrophilic salt on a mixture of water and an organic solvent is opposite to that of surfactant molecules,[7] which serve to increase the mutual solubility of water and the organic solvent by decreasing the interfacial energy.

Recently, we investigated the effect of the salt, sodium tetraphenylborate ($NaBPh_4$), which is composed of the hydrophilic cation Na^+ and hydrophobic anion BPh_4^-, on a mixture of deuterium oxide (D_2O) and 3-methylpyridine (3MP). Figure 1 shows the phase diagrams of D_2O/3MP/$NaBPh_4$ drawn from our previous and present experiments. The binary mixture of D_2O and 3MP shows closed-loop-type phase separation. When an antagonistic salt, $NaBPh_4$, is dissolved in the D_2O and 3MP mixture, the two-phase region shrinks as the amount of salt increases, and it disappears above 15 mmol/L;[8] thus, the mutual solubility of D_2O and 3MP increases in the presence of $NaBPh_4$ on the macroscopic scale. This result implies that the antagonistic salt can act as a surface-active agent in the D_2O and 3MP mixture. Moreover, a periodic structure with a characteristic length scale of hundreds to thousands of angstroms was observed by means of small-angle neutron scattering (SANS), even far from the phase separation point. In the D_2O-rich mixture in particular, an ordered-lamellar-phase (L_α phase) was found at a $NaBPh_4$ concentration of ≈85 mmol/L.[9]

These experimental observations are explained in the framework of the theory proposed by Onuki and Kitamura.[6,12,13] In their model, a charge-density-wave structure is induced by coupling the solvation effect and critical concentration fluctuations. In addition, they showed that hydrophilic and hydrophobic ions tend to adsorb near the interface between the water and the organic solvent. These ions act as an electric double layer at the interface, and reduce the interfacial tension between the water and the organic solvent.[13]

Although pairs of hydrophilic and hydrophobic ions play the role of a surface-active agent under certain conditions, the details of the formation mechanisms of a salt-induced ordered structure have not yet been clarified. As shown in Fig. 1(c), the composition and temperature ranges for the ordered-lamellar-structure are very narrow, suggesting that these structures are formed under a delicate balance among various interactions.

In the present study, we focused on the static and dynamic structures of the ordered-lamellar-structure in the mixture of D_2O/3MP/$NaBPh_4$ to understand how the ordered structure is stabilized. Neutron scattering techniques were employed to study the system because of the good scattering contrast

a)Electronic mail: sadakane@fc.ritsumei.ac.jp

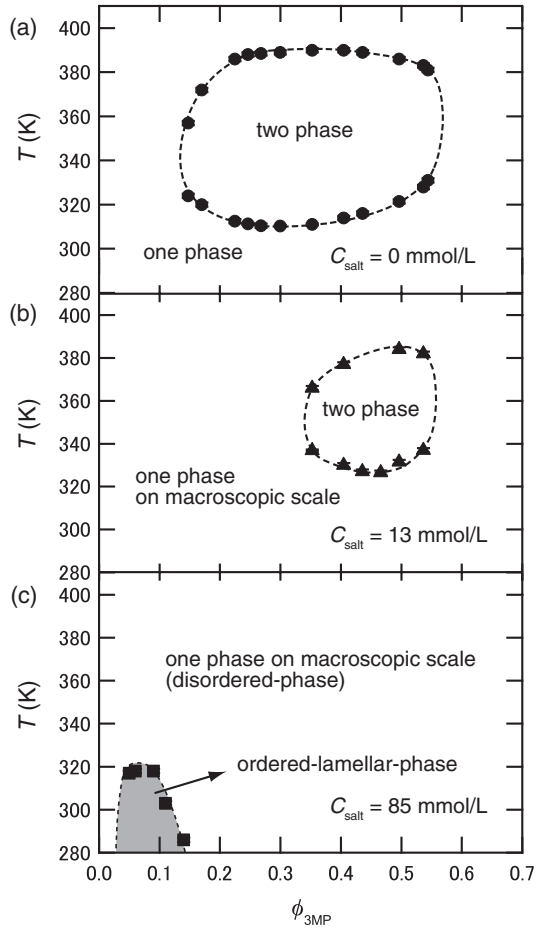

FIG. 1. Phase diagrams of D_2O/3MP/$NaBPh_4$ with salt concentrations of 0 mmol/L (a), 13 mmol/L (b), and 85 mmol/L (c). The horizontal axis ϕ_{3MP} indicates the volume fraction of 3MP, and the vertical axis is the temperature. The symbols in (a) and (b) show the cloud point obtained in previous research,[8,10] while the symbol in (c) shows the phase transition point of the disordered-phase and the ordered-lamellar-phase investigated through the present SANS measurements. The dotted lines are visual guides. Error bars are of a value ±1 K, which is the ambiguity in the estimation of the cloud point and the phase transition point.[11]

between D_2O and 3MP. The SANS results indicate various kinds of nanoscale structures are formed depending on conditions, and neutron spin echo (NSE) experiments confirm the membrane picture by measuring the collective dynamics of the system on the nanosecond timescale.

II. EXPERIMENTS

D_2O (deuterium oxide, 99.9% purity, EURISO-TOP), 3MP (3-methylpyridine, 99.5% purity, Aldrich), and $NaBPh_4$ (sodium tetraphenylborate, 99.5% purity, Aldrich) were mixed without further purification. The volume fraction of 3MP, $\phi_{3MP} = V_{3MP}/(V_{water} + V_{3MP} + V_{salt})$, was set at 0.09, 0.10, 0.12, and 0.13 (V_{water}, V_{3MP}, and V_{salt} denote the volumes of D_2O, 3MP, and $NaBPh_4$, respectively). The concentration of $NaBPh_4$ in the mixture, C_{salt}, was varied between 0 mmol/L and 300 mmol/L. We confirmed that the mass density of $NaBPh_4$ is 1.237 ± 0.007 g/ml. Based on the molecular weight of $NaBPh_4$ (342.22) and Na (23.00), the volume fraction of BPh_4^- ions (ϕ_{BPh}) is evaluated as $\phi_{BPh} = 2.77 \times 10^{-4} \times (C_{salt}[\text{mmol/L}])$. In addition, the van der Waals radius of BPh_4^- ion is evaluated as 4.9 Å. It is noted that 3MP is a weak base, and some molecules accept D^+ when D_2O is added. The base dissociation constant of 3MP, K_b, is 4.78×10^{-9} ($pK_b = 8.32$).[14] Additionally, we measured the pD value of a solution with $\phi_{3MP} = 0.09$ to be 9.43. According to these facts, the ratio of $3MPD^+$ to 3MP, [$3MPD^+$]/[3MP], is evaluated as 1.78×10^{-4} at 298.2 K. Therefore, in the present paper, we neglect the effect of the conjugated acid on the neutron scattering length density or electrostatic interactions between membranes.

The SANS measurements were performed using the NG3- and NG7-30 m SANS instruments at the National Institute of Standards and Technology (NIST) Center for Neutron Research (NCNR).[15] The wavelength of the incident neutron beam was 6 Å with a resolution of 14.2 % for NG3 and 12.4 % for NG7, and the scattered neutrons were collected with a two-dimensional ^{3}He detector placed at specific distances from the sample position: 1.3 m and 5.0 m for NG3, and 1.0 m and 6.5 m for NG7. The samples were kept in titanium cells with quartz windows. The sample thickness was 2 mm. A temperature-controlled chamber was used to regulate the sample temperature T with an accuracy of ± 0.1 K. The momentum transfer, $Q = 4\pi \sin\theta/\lambda$, was covered in the range from 8.6×10^{-3} Å^{-1} to 5.5×10^{-1} Å^{-1}, where λ and 2θ are the incident neutron wavelength and the scattering angle, respectively. The observed two-dimensional data were averaged azimuthally, and then corrected for transmission, background scattering, and the sample thickness to obtain absolute intensities in units of cm^{-1}.[16] The estimated incoherent scattering intensity was subtracted from the absolute intensity data.

The NSE experiments were carried out with the NG5-NSE spectrometer at the NCNR[17] and the iNSE spectrometer at the research reactor JRR-3 of the Japan Atomic Energy Agency.[18] The measured spatial and time domains for NG5-NSE were from 3×10^{-2} Å^{-1} to 2.5×10^{-1} Å^{-1} and from 0.05 ns to 15 ns, respectively, and those for iNSE were from 2×10^{-2} Å^{-1} to 1.5×10^{-1} Å^{-1} and from 0.16 ns to 16 ns, respectively. The sample was kept in a standard titanium cell with quartz windows for the NG5-NSE experiments, and in a quartz cell with a thickness of 4 mm for the iNSE experiments. The sample temperature T was regulated in a temperature-controlled chamber with an accuracy better than 0.1 K. The DAVE software package was used for data reduction of the NG5-NSE data.[19]

III. RESULTS

A. SANS studies with changing C_{salt}

Figure 2(a) shows the SANS profiles of D_2O/3MP/$NaBPh_4$ with changing C_{salt} at $\phi_{3MP} = 0.09$ and $T = 280.5$ K. When the concentration of $NaBPh_4$ is below 1 mmol/L, the SANS profile shows a monotonic decrease with increasing Q. The SANS profiles from binary D_2O/3MP are explained by employing the Ornstein–Zernike function,[20,21] which describes the concentration fluctuations of binary mixtures:

$$I_{OZ}(Q) = \frac{I_0}{1 + \xi^2 Q^2}, \quad (1)$$

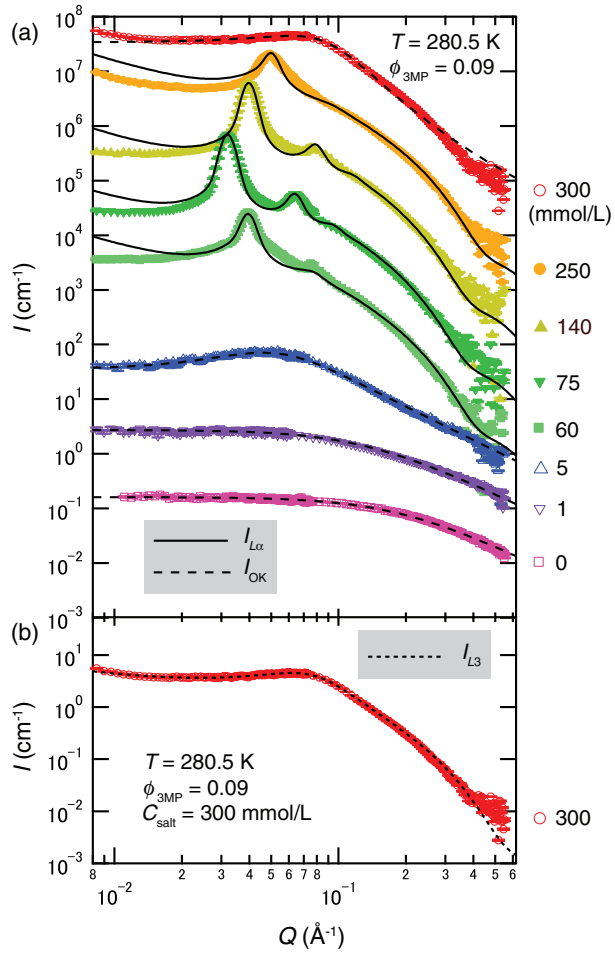

FIG. 2. (a) SANS profiles for D_2O/3MP/$NaBPh_4$ with changing C_{salt} at $\phi_{3MP} = 0.09$ and $T = 280.5$ K. Open and closed symbols indicate the data for the disordered- and ordered-lamellar-phase, respectively. The data at higher C_{salt} are shifted by a multiplication factor of 10 for better visualization. Dashed lines are the fit results given by Eqs. (1) and (2), and solid lines are those given by Eq. (7). (b) The same plot at $C_{salt} = 300$ mmol/L in absolute units. The dotted line is the fit result according to Eq. (4). In (a) and (b), error bars represent ±1 standard deviation.

where I_0 denotes the forward scattering intensity, which is proportional to the osmotic compressibility, and ξ the correlation length of the concentration fluctuation. The dashed lines in Fig. 2(a) for $C_{salt} = (0$ and $1)$ mmol/L are the fitting results according to Eq. (1). The distribution of D_2O and 3MP is well described in terms of the concentration fluctuations when C_{salt} is sufficiently small, i.e., $C_{salt} \leq 1$ mmol/L.

On the other hand, the SANS profile deviates from Eq. (1) when C_{salt} is above 5 mmol/L. This deviation originates from the growth of a peak followed by the formation of nanoscale structures. As investigated in the previous paper,[9] the SANS profiles show a sharp peak profile together with higher-order peaks in an ordered-lamellar-phase (L_α phase), and a single broad peak profile in a disordered phase. In the results of the present work, the ordered-lamellar-phase appears at 60 mmol/L $\leq C_{salt} \leq$ 250 mmol/L, while the disordered-phase is observed when C_{salt} is 5 mmol/L and 300 mmol/L.[22]

In order to analyze the SANS profiles in the disordered-phase, we employed the model scattering function for a mixture of water/organic solvent/salt, as proposed by Onuki and Kitamura.[12] On the basis of the Ginzburg–Landau theory, they derived the following function to explain the charge-density-wave structure:

$$I_{OK}(Q) = \frac{I_0}{1 + \left[1 - \gamma_p{}^2/(1 + \lambda_D{}^2 Q^2)\right]\xi^2 Q^2}, \tag{2}$$

where I_0 and ξ are the same parameters as in Eq. (1). The term λ_D denotes the Debye screening length,[23] and $\gamma_p(\gamma_p \geq 0)$ is a dimensionless parameter concerning the difference between the solubilities of cations and anions in water. It should be noted that Eq. (2) is equivalent to Eq. (1) when $\gamma_p = 0$. When an antagonistic salt is dissolved in the mixture of water and 3MP, γ_p increases to more than 1, and a peak due to the periodicity of a charge distribution (charge-density-wave structure) appears at finite Q. The peak position for $\gamma_p > 1$ is calculated as

$$Q_m = \frac{2\pi}{d} = \frac{\sqrt{\gamma_p - 1}}{\lambda_D}, \tag{3}$$

where d indicates the characteristic mean repeat distance. The dashed lines in Fig. 2(a) for $C_{salt} = 5$ mmol/L and 300 mmol/L indicate the fitting results according to Eq. (2). We found that the SANS profiles from the disordered-phase are explained well by Eq. (2) for $C_{salt} = 5$ mmol/L, but not for $C_{salt} = 300$ mmol/L at high Q. Table I summarizes the fit parameters derived from Eq. (2) for the mixture at $C_{salt} = 0$ mmol/L, 1 mmol/L, 5 mmol/L, and 300 mmol/L.

TABLE I. Best fit parameters in the disordered-phase of the D_2O/3MP/$NaBPh_4$ mixture ($\phi_{3MP} = 0.09$ and $T = 280.5$ K) according to Eq. (2).

C_{salt} (mmol/L)	I_0 (cm^{-1})	ξ (Å)	γ_p	λ_D (Å)
0	0.161 ± 0.001	5.4 ± 0.1	0	...
1	0.273 ± 0.002	7.5 ± 0.1	0	...
5	0.355 ± 0.007	11.2 ± 0.3	2.89 ± 0.14	29.9 ± 1.3
300	3.411 ± 0.022	30.5 ± 0.3	1.07 ± 0.01	4.3 ± 0.5

The fitting result obtained using Eq. (2) shows a slight deviation from the SANS profile for $C_{salt} = 300$ mmol/L at $Q \geq 0.3$ Å^{-1}. This deviation should reflect the influence of the form factor of the molecular arrangement near the interfaces of the system on a scale of 10 Å to 20 Å. We assume that a thin layer, composed mainly of 3MP, constitutes the internal structure. Here, we employ a model scattering function for the binary sponge (L_3) structure.[24–27] The model scattering function for the sponge structure of a surfactant solution is given as[25,27]

$$I_{L3}(Q) = \frac{\phi_{3MP} + \phi_{BPh}}{\pi r_d{}^2 \delta} P_{L3}(Q) S_{L3}(Q), \tag{4}$$

with the form factor derived from randomly oriented disks of membranes

$$P_{L3}(Q) = 4\left(\pi r_d{}^2 \Delta\rho\right)^2 \frac{[1 - \cos(\delta Q)\exp(-\delta^2 Q^2/32)]/Q^2}{r_d{}^2 Q^2 + 2\exp\left(-r_d{}^2 Q^2/6\right)}, \tag{5}$$

and the structure factor

$$S_{L3}(Q) = 1 + \frac{C_1 \arctan(\xi_{io} Q/2)}{Q} + \frac{C_2}{1/\xi_c{}^2 + (Q - 2\pi/d)^2}$$
$$\approx 1 + \frac{C_1 \pi}{2Q} + \frac{C_2}{1/\xi_c{}^2 + (Q - 2\pi/d)^2}, \quad (6)$$

where r_d the radius of gyration of a disk membrane, $\Delta\rho$ the difference in scattering length density distribution between membrane and bulk water, δ the thickness of membrane, ξ_{io} the inside–outside correlation length, which reflects the membrane scale,[24] and ξ_c the correlation length of cells. The terms C_1 and C_2 are constants. In the fitting procedure, the term $\arctan(\xi_{io} Q/2)$ in Eq. (6) was approximated as $\pi/2$ by assuming that the value of ξ_{io} is sufficiently large. As shown in Fig. 2(b), the SANS profile for the mixture at C_{salt} = 300 mmol/L is well explained by Eq. (4) including the high-Q region, with the fitting parameters being $d = 92 \pm 1$ Å, $\delta = 16 \pm 1$ Å, $r_d = 6.7 \pm 0.7$ Å, $\xi_c = 25.0 \pm 0.8$ Å, and $\Delta\rho = (4.7 \pm 0.8) \times 10^{10}$ cm^{-2}.

The SANS profiles obtained from the ordered-lamellar-phase are analyzed according to the model scattering function for lamellar structures in surfactant systems, as proposed by Nallet *et al.*, as[28]

$$I_{L\alpha}(Q) = \frac{2\pi P_{L\alpha}(Q) S_{L\alpha}(Q)}{dQ^2}, \quad (7)$$

with the form factor of the membrane

$$P_{L\alpha}(Q) = \frac{2(\Delta\rho)^2}{Q^2}\left[1 - \cos(\delta Q)\exp\left(-\frac{1}{2}\tau^2 Q^2\right)\right] \quad (8)$$

and the structure factor

$$S_{L\alpha}(Q) = 1 + 2\sum_{n=1}^{N-1}\left(1 - \frac{n}{N}\right)\cos\left(\frac{dnQ}{1 + 2\Delta Q^2 d^2 g(n)}\right)$$
$$\times \exp\left[-\frac{\Delta Q^2 d^2 n^2 + 2d^2 g(n) Q^2}{2(1 + 2\Delta Q^2 d^2 g(n))}\right]$$
$$\times \frac{1}{\sqrt{1 + 2\Delta Q^2 d^2 g(n)}}, \quad (9)$$

where τ denotes the membrane thickness distribution, which could be fixed at $\delta/4$ as the cases of surfactant membranes,[28,29] N the number of layers, and ΔQ the instrumental resolution. The value of N is fixed at 500 since $S_{L\alpha}(Q)$ is almost independent of N when N is larger than a certain value, i.e., $N = 100$.[30] The correlation function of fluctuating membranes $g(n)$ is given by

$$g(n) = \frac{\eta}{4\pi^2}\left[\ln(\pi n) + 0.5772\right], \quad (10)$$

$$\eta = \frac{Q_m{}^2 k_B T}{8\pi\sqrt{K\bar{B}}}, \quad (11)$$

where η represents the Caillé parameter, which reflects the regularity of membranes,[31] Q_m denotes the position of the first-order Bragg peak, k_B the Boltzmann constant, K the bulk bending modulus ($K = \kappa/d$, where κ denotes the bending modulus for a single membrane), and $\bar{B}$ the layer compressibility at constant surfactant and oil chemical potentials (i.e., at constant 3MP and salt chemical potentials, in the present case). A smaller value of η indicates better periodicity of the lamellar structure. The width of the instrumental resolution function ΔQ is given by[29]

$$\Delta Q^2 = \frac{Q^2}{8\ln 2}\left(\frac{\Delta\lambda}{\lambda}\right)^2 + \frac{(2\pi)^2}{12\lambda^2}\left[3\frac{R_1{}^2}{L_1{}^2} + 3\frac{R_2{}^2}{L'^2} + \frac{(\Delta R)^2}{L_2^2}\right], \quad (12)$$

where R_1 and R_2 denote the radii of the source and sample aperture (50.00 mm and 12.70 mm, respectively), ΔR the detector resolution (5 mm), L_1 and L_2 the incident and scattered flight path lengths, respectively, and $L' = L_1 L_2/(L_1 + L_2)$. These parameters are defined for the experimental setup of the SANS measurements. Although Eq. (7) was proposed to explain the lamellar structure in surfactant systems, it has been applied to investigate the structural features of the present system.[9] The fitting results according to Eq. (7) are shown in Fig. 2(a) with solid lines for the SANS profiles of the samples with $NaBPh_4$ concentration between 60 mmol/L and 250 mmol/L, and the curves reproduce the experimental results well. The fit parameters d, η, and δ are summarized in Table II.

TABLE II. Best fit parameters in the ordered-lamellar-phase of D_2O/3MP/$NaBPh_4$ (ϕ_{3MP} = 0.09 and T is around 281 K) according to Eq. (7).

C_{salt} (mmol/L)	d (Å)	η	δ (Å)
60	157.3 ± 0.2	0.44 ± 0.01	14 ± 4
75	194.3 ± 0.3	0.19 ± 0.01	16 ± 2
85	195.6 ± 0.2	0.20 ± 0.01	16 ± 3
120	172.2 ± 0.2	0.20 ± 0.01	16 ± 2
140	156.7 ± 0.2	0.23 ± 0.01	15 ± 2
160	145.4 ± 0.3	0.38 ± 0.01	15 ± 5
180	140.9 ± 0.1	0.41 ± 0.01	14 ± 3
200	141.8 ± 0.2	0.48 ± 0.01	14 ± 3
250	123.8 ± 0.4	0.65 ± 0.01	13 ± 4

From the analyses performed using Eqs. (4) and (7), the existence of membrane structures is confirmed in both the sponge phase and ordered-lamellar-phase. Here, it could be reasonable to speculate that the D_2O-rich and 3MP-rich domains behave as bulk water and membranes, respectively. Since BPh_4^- is hydrophobic,[32] most BPh_4^- ions should exist in 3MP-rich domains rather than in bulk water. The 3MP-rich membranes are stacked regularly, and the nanostructures, i.e., sponge structure and ordered-lamellar-structure, are generated.

Figure 3 shows the C_{salt} dependence of the fit parameters, d, δ, η, and $\Delta\rho$ for the mixture of D_2O/3MP/$NaBPh_4$ (ϕ_{3MP} = 0.09). The temperature is 281.8 K for the mixture at C_{salt} = 85 mmol/L and 280.5 K in the other cases. Here, we confirmed that the effect of the temperature difference, i.e., 281.8 K and 280.5 K, on the SANS profile at C_{salt} = 85 mmol/L is negligible. In Figs. 3(a), 3(c), and 3(d), the data for the sponge phase derived from Eq. (4) are also shown as open symbols. The characteristic maximum value of the mean

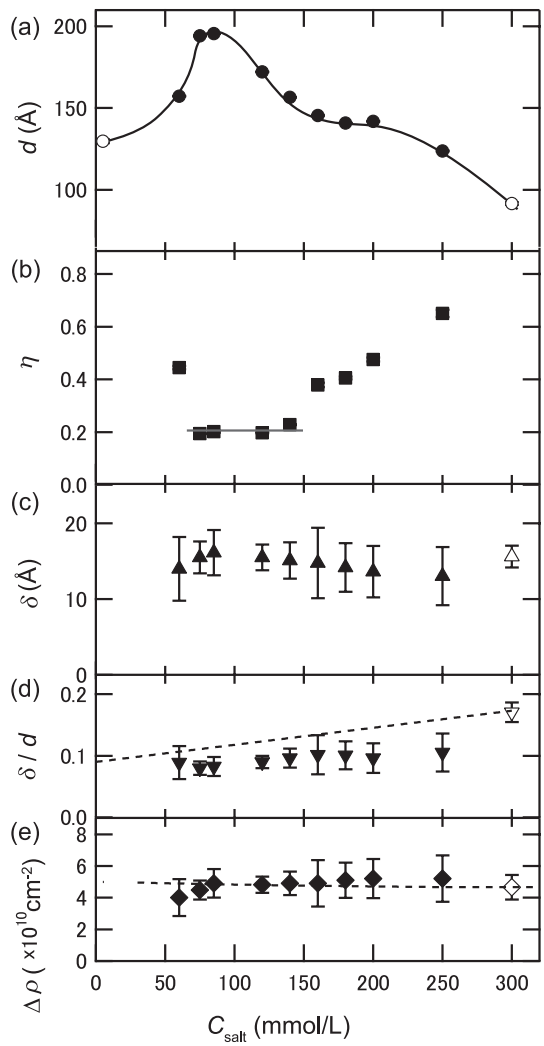

FIG. 3. C_{salt} dependence of the fit parameters, d, δ, η, and $\Delta\rho$ for the mixture of D_2O/3MP/$NaBPh_4$ ($\phi_{3MP} = 0.09$). The temperature is 281.8 K for the mixture at $C_{salt} = 85$ mmol/L and 280.5 K in the other cases. The open and closed symbols indicate the data in the disordered-phase and the ordered-lamellar-phase, respectively. Error bars represent ±1 standard deviation. (a) The mean repeat distance d. The solid line is a visual guide. (b) The Caillé parameter η. The solid line is a visual guide for the data at $75\,\text{mmol/L} \le C_{salt} \le 140\,\text{mmol/L}$, where η shows relatively small values. (c) The membrane thickness δ. (d) The C_{salt} dependence of δ/d. The dashed line indicates the estimated values, $(\delta/d)_{calc}$, according to Eq. (13). (e) The scattering length density difference between the membrane and the bulk water, $\Delta\rho$. The dashed line indicates the values of $\Delta\rho_{calc}$ according to Eq. (14).

repeat distance, d, is observed at $C_{salt} \approx 85$ mmol/L. On the other hand, η has its minimum around $C_{salt} = 75$ mmol/L to 140 mmol/L. Figure 3(d) shows the C_{salt} dependence of δ/d. Here, $(\delta/d)_{calc}$ is evaluated by assuming that the membranes are composed of 3MP and BPh_4^- ions, and that the morphology of the sponge and ordered-lamellar-structure follows the ideal dilution relation:

$$(\delta/d)_{calc} = \phi_{3MP} + \phi_{BPh}. \tag{13}$$

In Eq. (13), the volume fraction of Na^+ in 3MP-rich domains is ignored, since this magnitude is sufficiently small compared with that of BPh_4^-.[32] The magnitudes of δ/d and $(\delta/d)_{calc}$ are close enough, and this result supports the idea that the membranes are composed of 3MP-rich domains and ions. A small discrepancy between δ/d and $(\delta/d)_{calc}$ may originate from the partial mixing of D_2O and 3MP molecules. Figure 3(e) shows the C_{salt} dependence of $\Delta\rho$ and $\Delta\rho_{calc}$, which is evaluated from

$$\Delta\rho_{calc} = \rho_{D_2O} - \left(\frac{\phi_{3MP}}{\phi_{3MP} + \phi_{BPh}}\rho_{3MP} + \frac{\phi_{BPh}}{\phi_{3MP} + \phi_{BPh}}\rho_{BPh}\right), \tag{14}$$

where $\rho_{D_2O}(6.4 \times 10^{10}\text{cm}^{-2})$, $\rho_{3MP}(1.4 \times 10^{10}\text{cm}^{-2})$, and $\rho_{BPh}(2.1 \times 10^{10}\text{cm}^{-2})$ denote the scattering length densities of D_2O, 3MP, and BPh_4^- ions, respectively, for 6 Å neutrons. The coincidence of $\Delta\rho$ and $\Delta\rho_{calc}$ suggests that strong scattering occurs because of the spatial distribution between bulk water composed of D_2O-rich domains and the membrane composed of 3MP-rich domains and BPh_4^- ions.

In this manner, the fitting results give a reasonable set of structural parameters, and they validate the application of the aforementioned models to the system. Because the Nallet model originally assumes a regular stacking of surfactant layers in water, the fitting results confirm the picture that planar 3MP-rich domains are stacked regularly in water.

B. SANS studies with changing T and ϕ_{3MP}

Next, the temperature and ϕ_{3MP} dependencies of the nanoscale structures are investigated for a fixed C_{salt} value of 85 mmol/L. Figure 4 shows the SANS profiles of the D_2O/3MP/$NaBPh_4$ system ($\phi_{3MP} = 0.09$, $C_{salt} = 85$ mmol/L) with changing temperature. The open and closed symbols indicate the data for the disordered-phase and ordered-lamellar-phase, respectively. The dotted and solid lines in Fig. 4(a) are the fitting results according to Eqs. (4) and (7), respectively. The SANS profiles from the disordered-phase are well reproduced by Eq. (4), whereas the profiles from the ordered-lamellar-phase are well described by Eq. (7). Therefore, it is concluded that the membrane structure is formed in both the disordered-phase and ordered-lamellar-phase.

At $T = 340.8$ K, the disordered-phase is confirmed from the broad peak profile, and the peak position Q_m shifts to lower Q values with decreasing temperature. As shown in Fig. 4(b), the sample is two phase coexistence at $T \approx 318$ K: a single broad peak from the disordered-phase is observed in the lower part of the sample, and a sharp peak profile, from the ordered-lamellar-phase, is observed in the upper part. This evidence clearly shows that a 1st-order phase transition occurs at $T \approx 318$ K. A further decrease in temperature makes the system uniform macroscopically, and the SANS profile shows multiple peaks resulting from the formation of the lamellar structure.

Figure 5 shows the temperature dependencies of d, η, and δ/d, both in the disordered-phase derived from Eq. (4) (open symbols) and the ordered-lamellar-phase from Eq. (7) (closed symbols). As shown in Fig. 5(a), d increases with decreasing temperature for all the samples. On the other hand, η decreases with decreasing temperature (see Fig. 5(b)). Thus, the regularity of the membrane structure increases with decreasing temperature. As shown in Fig. 5(c), the magnitudes of δ/d and $(\delta/d)_{calc}$ derived from Eq. (13) are of the same order for the mixture at $C_{salt} = 85$ mmol/L and $\phi_{3MP} = 0.09$.

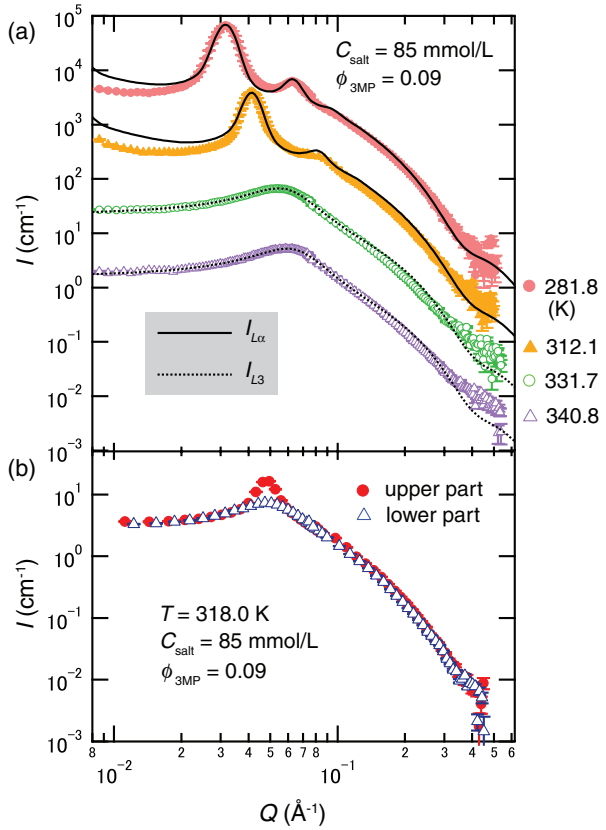

FIG. 4. (a) Temperature dependence of the SANS profiles for D_2O/3MP/$NaBPh_4$ (C_{salt} = 85 mmol/L and ϕ_{3MP} = 0.09). The data at lower temperatures are shifted by a multiplication factor of 10 for better visualization. The open and closed symbols indicate the data for the disordered-phase and the ordered-lamellar-phase, respectively. The dotted and solid lines show the fitting results according to Eqs. (4) and (7), respectively. (b) SANS profiles for D_2O/3MP/$NaBPh_4$ at C_{salt} = 85 mmol/L, ϕ_{3MP} = 0.09, and T = 318.0 K. Under these conditions, the mixture separates into two phases: the lower part of the sample is in the disordered-phase, while the upper part is in the ordered-lamellar-phase.

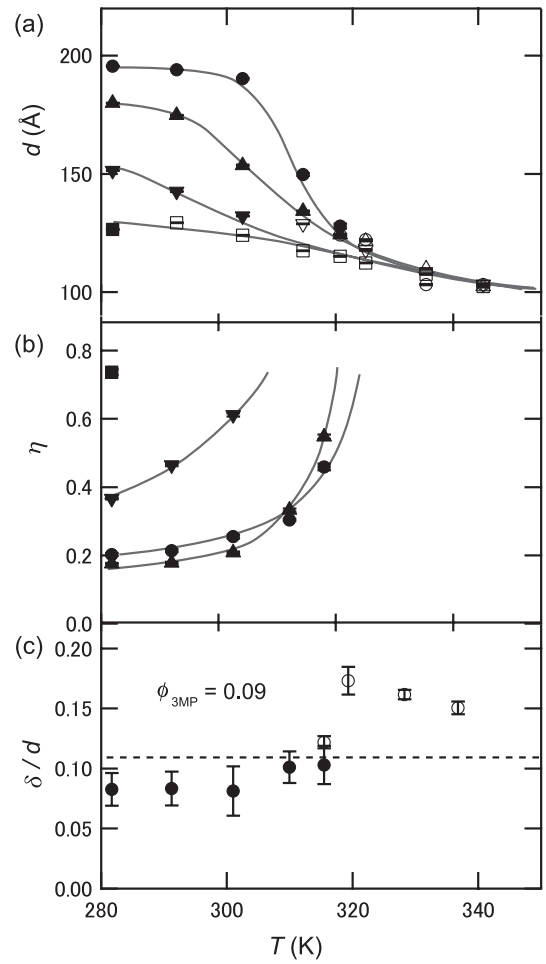

FIG. 5. Temperature dependence of the fit parameters, d, η, and δ/d for the mixture of D_2O/3MP/$NaBPh_4$ (C_{salt} = 85 mmol/L) both in the disordered-phase (open symbols) given by Eq. (4) and the ordered-lamellar-phase (closed symbols) given by Eq. (7). Circles, triangles, inverted triangles, and squares indicate the data for ϕ_{3MP} = 0.09, 0.10, 0.12, and 0.13, respectively. Solid lines in (a) and (b) are visual guides. (a) The temperature dependence of d. (b) The temperature dependence of η. (c) The temperature dependence of δ/d. The dashed line indicates the estimated values, $(\delta/d)_{calc}$, according to Eq. (13).

Figure 6(a) exhibits the ϕ_{3MP} dependence of d at two different temperatures: the open and closed symbols indicate the data for T = 340.8 K (disordered-phase) and T = 281.8 K (ordered-lamellar-phase), respectively. At T = 340.8 K, d is almost independent of ϕ_{3MP}, with a value of about d = 107 Å. This indicates that the values of δ/d do not follow the ideal dilution relation, $\delta/d = \phi_{3MP} + \phi_{BPh}$, in the disordered-phase. On the other hand, d increases with decreasing ϕ_{3MP} at T = 281.8 K. This behavior is similar to that of the smectic lamellar structure in surfactant systems, which follows the ideal dilution relation.[33] Figure 6(b) shows the ϕ_{3MP} dependence of η at T = 281.8 K. η reaches a minimum value around a certain value of ϕ_{3MP}: ϕ_{3MP} = 0.1 in this sample. It is noteworthy that this tendency is also observed in some surfactant mixtures. In the mixture of water/octane/nonionic polyoxyethylene surfactant ($C_{12}E_5$), for example, the minimum η value is observed at around ϕ = 0.5 (where ϕ denotes the volume fraction of oil) since the layer compressibility $\bar{B}$ attains a maximum value at ϕ = 0.5 in this system.[34] Figure 6(c) shows the ϕ_{3MP} dependence of δ/d. With increasing ϕ_{3MP}, δ/d slightly increases at T = 281.8 K, whereas, slightly decreases at T = 340.8 K. The magnitudes of δ/d and $(\delta/d)_{calc}$ derived from Eq. (13) are of the same order for the mixture at ϕ_{3MP} = 0.09, 0.10, 0.12, and 0.13 (see Fig. 6(c)).

C. NSE studies with changing T and ϕ_{3MP}

As shown above, the disordered-structure (i.e., charge-density-wave structure and sponge structure) and ordered-lamellar-structure are observed in the mixture of D_2O/3MP upon the addition of $NaBPh_4$. So far, the dynamical behaviors of surfactant monolayers or bilayers have been investigated both theoretically and experimentally.[35–44] The stability of such membranes has been discussed considering the bending elastic properties through the Helfrich bending Hamiltonian.[45] We compare the dynamical properties of the newly discovered nanostructures in D_2O/3MP/$NaBPh_4$ with the theory for surfactant membranes.

The dynamical properties of the system were investigated by means of NSE. Figure 7(a) shows the normalized intermediate correlation function $I(Q, t)/I(Q, 0)$ for the mixture at

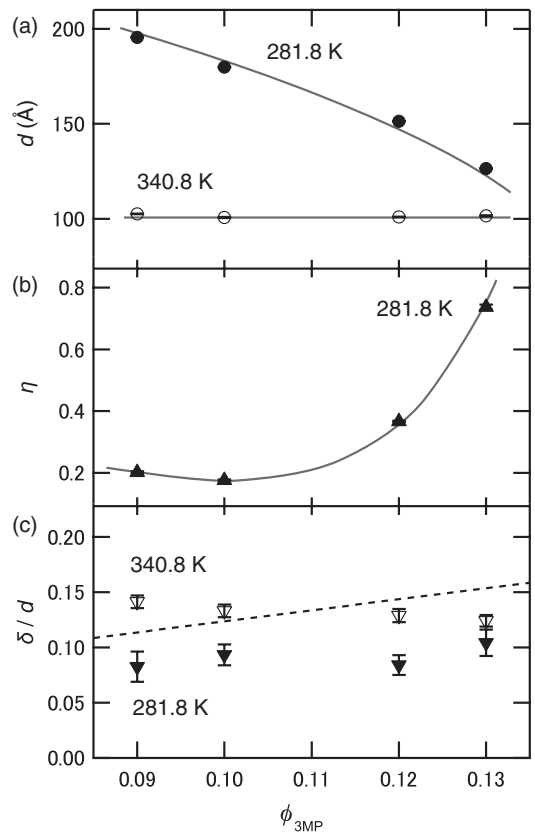

FIG. 6. ϕ_{3MP} dependence of d, η, and δ/d for the mixture of D_2O/3MP/$NaBPh_4$ (C_{salt} = 85 mmol/L) both in the disordered-phase (open symbols) given by Eq. (4) and the ordered-lamellar-phase (closed symbols) given by Eq. (7). Solid lines in (a) and (b) are visual guides. (a) ϕ_{3MP} dependence of d. (b) ϕ_{3MP} dependence of η. (c) ϕ_{3MP} dependence of δ/d. The dashed line indicates the estimated values, $(\delta/d)_{calc}$, according to Eq. (13).

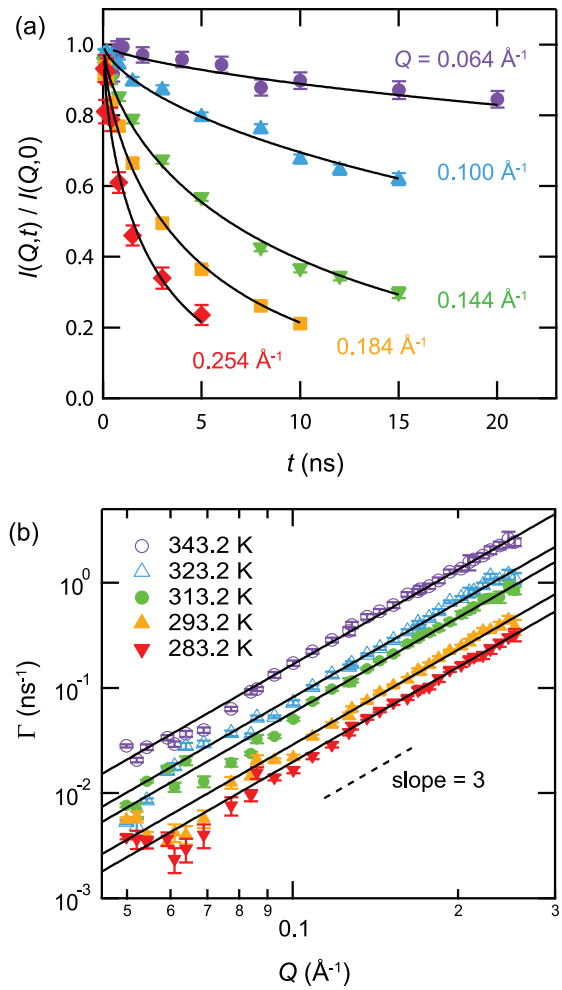

FIG. 7. (a) Normalized intermediate correlation functions $I(Q, t)/I(Q, 0)$ for the mixture of D_2O/3MP/$NaBPh_4$ at C_{salt} = 85 mmol/L, ϕ_{3MP} = 0.09, and T = 293.2 K. The solid lines indicate the fitting results according to Eq. (15). (b) Q dependence of the relaxation rate Γ obtained from the fit of $I(Q, t)/I(Q, 0)$ according to Eq. (15) for the mixture of D_2O/3MP/$NaBPh_4$ at C_{salt} = 85 mmol/L, ϕ_{3MP} = 0.09, and 283.2 K $\leq T \leq$ 343.2 K. The open and closed symbols indicate the data for the disordered-phase (sponge phase) and the ordered-lamellar-phase, respectively. The solid lines are the fitting results to Eq. (16). Error bars represent ±1 standard deviation.

C_{salt} = 85 mmol/L, ϕ_{3MP} = 0.09, and T = 293.2 K, which is the ordered-lamellar-phase of the system. In the case of a fluctuating surfactant membrane, the intermediate correlation function $I(Q, t)/I(Q, 0)$ is expressed by using the stretched exponential function as follows:[39,41]

$$\frac{I(Q,t)}{I(Q,0)} = \exp[-(\Gamma t)^{2/3}], \tag{15}$$

where Γ denotes the relaxation rate. Figure 7(b) shows the Q dependence of Γ. The single membrane fluctuation model proposed by Zilman and Granek (ZG)[39] gives the Q^3 relation of Γ as

$$\Gamma = 0.025\gamma_k \left(\frac{k_B T}{\kappa_{NSE}}\right)^{1/2} \frac{k_B T}{\eta_{vis}} Q^3, \tag{16}$$

where κ_{NSE} and η_{vis} denote the bending modulus of the membrane and the viscosity of the surrounding medium, respectively. The factor γ_k originates from the averaging over the angle between the wave vector and the membrane surface in the calculation of $I(Q, t)$. In the present analysis, we set $\gamma_k = 1$ for simplicity. For the value of η_{vis}, we used the following values for the viscosity of D_2O: 1.676 mPa·s (283.2 K), 1.250 mPa·s (293.2 K), 1.110 mPa·s (298.2 K), 0.786 mPa·s (313.2 K), 0.651 mPa·s (323.2 K), 0.535 mPa·s (335.1 K), and 0.474 mPa·s (343.2 K).[46] Throughout the observed Q range (i.e., 3.0 × 10^{-2} Å^{-1} $\leq Q \leq$ 2.5 × 10^{-1} Å^{-1}) and temperature range (i.e., 283.2 K $\leq T \leq$ 343.2 K), $I(Q, t)/I(Q, 0)$ is well fitted by Eq. (15), and Γ follows Eq. (16).

It should be noted that the Q dependence of Γ shows a slight deviation from Eq. (16) around Q = 0.07 Å^{-1} due to the so-called de Gennes narrowing. At the length scales of the inter-layer distance, the relative motion of the membranes becomes slower, and the apparent Γ becomes smaller. The appropriate Q range of the ZG model is limited by the inter-lamellar distance (low-Q limit) and the membrane thickness (high-Q limit). Further, it is noted that the ZG model is based on the assumption that a membrane fluctuates freely without being affected by long-range intermembrane interactions. In the present system, the long-range electrostatic repulsion dominates the lamellar structure, as will be shown in Sec. IV. Nonetheless, the dynamical properties in this system can also be described well by Eqs. (15) and (16). This fact may suggest that the principal behavior of the membrane fluctuation of this

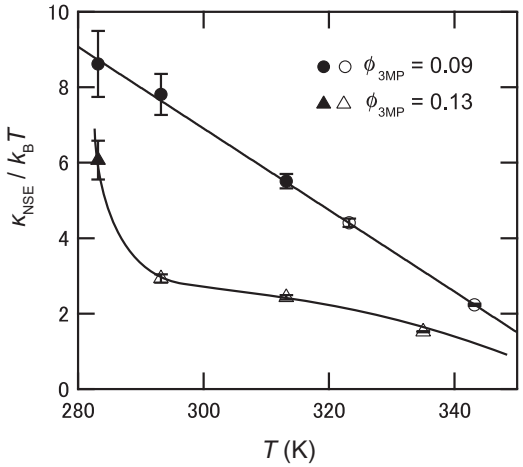

FIG. 8. Temperature dependence of κ_{NSE}/k_BT according to Eq. (16). The closed and open symbols indicate the data for the ordered-lamellar-phase and disordered-phase, respectively. The solid lines are visual guides. Error bars represent ±1 standard deviation.

system in both the sponge phase and ordered-lamellar-phase is less affected by the existence of a long-range intermembrane interaction.

Figure 8 shows the temperature dependence of κ_{NSE}/k_BT according to Eq. (16) for the mixtures of $C_{salt} = 85$ mmol/L at various ϕ_{3MP} from 0.09 to 0.13. κ_{NSE}/k_BT decreases with increasing temperature. Here, it is noted that the value of κ_{NSE} according to Eq. (16) in surfactant systems deviates from the actual value because of the difference between the viscosity of water η_{vis} and the effective viscosity of bulk water near membranes: in many cases, κ_{NSE} approaches the reasonable value when η_{eff} is substituted with $\eta_{eff} \approx 3\eta_{vis}$.[41,47–50] Similarly, the values of κ_{NSE}/k_BT in the present case may deviate from the reasonable values. In addition, the long-range electrostatic repulsion between membranes can suppress their fluctuation,[23] and this increases the value of κ_{NSE} from the actual value.

IV. DISCUSSION

In this study, we showed that an antagonistic salt $NaBPh_4$ in a mixture of D_2O and 3MP induces nanostructures, i.e., the disordered-structure and the ordered-lamellar structure. Around $T = 281$ K, the SANS profile at $C_{salt} = 5$ mmol/L is explained by the function describing the charge-density-wave structure (Eq. (2)), and the profile at $C_{salt} = 300$ mmol/L is modeled by the scattering function of the sponge phase of surfactant solutions (Eq. (4)). The boundary between D_2O-rich and 3MP-rich domains is vague in the charge-density-wave phase, whereas the boundary is sharp and membranes are formed in the sponge phase. In addition, the SANS profiles for the mixture at $60\,\text{mmol/L} \le C_{salt} \le 250$ mmol/L are well explained by the model function of a lamellar structure in surfactant mixtures[28] (see Eq. (7)). In both the sponge phase and the ordered-lamellar-phase, 3MP-rich domains exist as planar membranes and their dynamics are well explained as fluctuating membranes.

Figure 9(a) describes the scattering length density distribution obtained to describe the SANS profile for

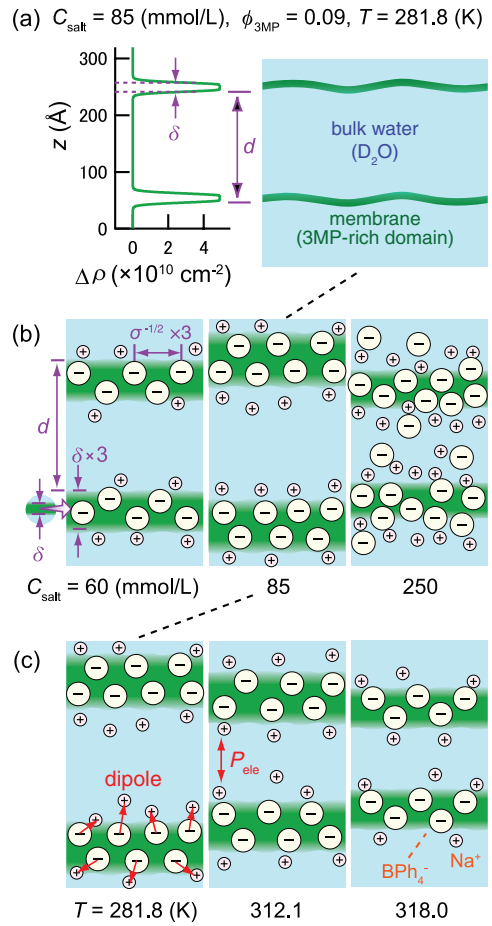

FIG. 9. (a) Scattering length density distribution obtained to describe the SANS profile for D_2O/3MP/$NaBPh_4$ at $C_{salt} = 85$ mmol/L, $\phi_{3MP} = 0.09$, and $T = 281.8$ K (left), and the schematic illustration of the system, indicating the membrane structure mainly composed of 3MP according to the results of SANS and NSE measurements (right). The vertical axis indicates the distance normal to the layers. (b) Schematic illustration indicating the C_{salt} dependence of d, δ, and the distribution of ions. (c) Schematic illustration indicating the temperature dependence of d, δ, and the distribution of ions. In (b) and (c), the scale of the membrane thickness δ and the van der Waals radius of BPh_4^- ion (4.9 Å, see Sec. II) are expanded to three times their original size to facilitate visualization. Additionally, the ionic radius of Na^+ (0.95 Å[51]) is expanded to eight times its original size. In (c), the dipole moment arising from Na^+ and BPh_4^- ion pairs, and the electrostatic repulsion between membranes, P_{ele}, are also described.

D_2O/3MP/$NaBPh_4$ at $C_{salt} = 85$ mmol/L, $\phi_{3MP} = 0.09$, and $T = 281.8$ K (left), and the schematic illustration of the system, indicating the membrane structure mainly composed of 3MP according to the results of SANS and NSE measurements (right). Figure 9(b) models the ordered-lamellar-structure at $\phi_{3MP} = 0.09$ around $T = 281$ K with changing C_{salt}. The membrane is composed of 3MP-rich domains and BPh_4^- ions. Na^+ ions are distributed around the surface of the membrane. d increases with increasing C_{salt} up to 85 mmol/L, but decreases above C_{salt} is 85 mmol/L. Figure 9(c) models the ordered-lamellar-structure at $C_{salt} = 85$ mmol/L and $\phi_{3MP} = 0.09$ with changing temperature. With increasing temperature, d decreases.

In this section, we discuss the origin of the planar membrane formation and the lamellar structure that does not contain any surfactant molecules or polymers.

A. Formation mechanisms of the membrane

According to the theoretical consideration of Onuki and Kitamura, a pair of hydrophilic and hydrophobic ions tends to adsorb at the interface between domains of water and organic solvent.[12,13] Then, macrophase separation is inhibited to satisfy the charge neutrality in each domain. This expectation is consistent with the experimental result, which shows that the two-phase region in the mixture of D_2O/3MP/$NaBPh_4$ shrinks with an increasing amount of $NaBPh_4$ (see Fig. 1). Therefore, a certain number of Na^+ and BPh_4^- ion pairs should adsorb around the interface between D_2O-rich and 3MP-rich domains: the majority of Na^+ ions are distributed in D_2O-rich domains, whereas BPh_4^- ions are distributed in 3MP-rich domains.

As shown in Table I, the magnitudes of I_0 and ξ increase with increasing C_{salt}. This indicates that the contrast between D_2O-rich and 3MP-rich domains and/or the number of separated domains increases with increasing salt concentration. In other words, microphase separation is enhanced with increasing C_{salt}, in contrast to the fact that macrophase separation is suppressed. The microphase separated domains are stretched owing to the entropic effect of ions, that is, the translational entropy of Na^+ and BPh_4^- ions distributed around the interface between D_2O-rich and 3MP-rich domains increases with increasing interfacial area. In the present case, the stretched 3MP-rich domain behaves as a membrane.

B. The stabilization of the ordered-lamellar-structure

As shown in Fig. 9, the membrane surfaces are negatively charged because of the BPh_4^- ions in 3MP-rich domains. This picture is analogous to ionic surfactant membranes, and the intermembrane interaction free energy per unit surface area could be assumed following that for ionic surfactant mixtures:[23,33,52]

$$f_{\mathrm{int}} = f_{\mathrm{hyd}} + f_{\mathrm{ele}} + f_{\mathrm{vdW}} + f_{\mathrm{Hel}}, \tag{17}$$

where f_{hyd} denotes the free energy arising from the hydration structures of surface charges, f_{ele} the free energy of the electrostatic interaction (so-called electrostatic double-layer repulsion[23]), f_{vdW} the free energy of the van der Waals interaction, and f_{Hel} the free energy arising from the steric interaction (Helfrich interaction[45]).

It is reasonable to neglect the effect of f_{hyd} when d is larger than 30 Å, because this effect is known as short-ranged.[53]

f_{ele} is evaluated from the electrostatic pressure between neighboring membranes, P_{ele}, arising from the "entropic" effect of Na^+ ions in D_2O-rich domains, as[23,33]

$$P_{\mathrm{ele}} = \frac{k_{\mathrm{B}}T\pi^3\alpha^2\ell_{\mathrm{B}}\sigma^2}{2\{1+\pi\ell_{\mathrm{B}}\alpha\sigma(d-\delta)\}^2}, \tag{18}$$

$$f_{\mathrm{ele}} = -\frac{1}{2}\int_{\infty}^{d} P_{\mathrm{ele}}\, d(d) \approx \frac{k_{\mathrm{B}}T\pi^2\alpha\sigma}{4\{1+\pi\alpha\sigma\ell_{\mathrm{B}}(d-\delta)\}}, \tag{19}$$

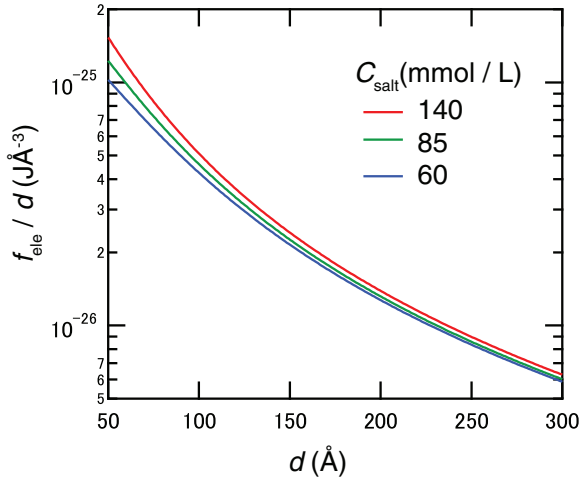

FIG. 10. The d dependences of f_{ele}/d evaluated from Eq. (19) for the mixture at $C_{\mathrm{salt}} = 60$ mmol/L, 85 mmol/L, or 140 mmol/L, $\phi_{3\mathrm{MP}} = 0.09$, and $T = 280.5$ K. α is set to 1 for simplicity.

where ℓ_{B} denotes the Bjerrum length ($\ell_{\mathrm{B}} \approx 7$ Å), σ the surface density of BPh_4^- ions, and α a dimensionless parameter, which is set to $\alpha = 1$ if all Na^+ ions are dissociated and exist only in water-rich domains (otherwise $0 \le \alpha < 1$). By assuming that all BPh_4^- ions exist at the interface between D_2O-rich domains and 3MP-rich domains, σ is given by

$$\sigma = \frac{1}{2}C_{\mathrm{salt}}N_{\mathrm{A}}d, \tag{20}$$

where N_{A} denotes Avogadro's number. The C_{salt} and temperature dependence of σ according to Eq. (20) is shown in Fig. 11. If we set $\alpha = 1$, for simplicity, the typical value of f_{ele} is evaluated as $f_{\mathrm{ele}} = 2.3 \times 10^{-24}$ JÅ^{-2} for the mixture at $C_{\mathrm{salt}} = 85$ mmol/L, $\phi_{3\mathrm{MP}} = 0.09$, and $T = 281.8$ K. Figure 10 shows the d dependence of f_{ele}/d evaluated from Eq. (19) for the mixture at $C_{\mathrm{salt}} = 60$ mmol/L, 85 mmol/L, or 140 mmol/L, $\phi_{3\mathrm{MP}} = 0.09$, and $T = 280.5$ K. α is set to 1 for simplicity. Here, the factor $1/d$ represents the number of the membranes per unit length. The results show that f_{ele}/d decrease with increasing d, that is, P_{ele} acts as a repulsive interaction.

f_{vdW} is approximately given as

$$f_{\mathrm{vdW}} \approx \frac{-k_{\mathrm{B}}T}{12\pi}\left\{\frac{1}{(d-\delta)^2} + \frac{1}{(d+\delta)^2} - \frac{2}{d^2}\right\}. \tag{21}$$

The typical value is $f_{\mathrm{vdW}} = -1.1 \times 10^{-28}$ JÅ^{-2} for the mixture at $C_{\mathrm{salt}} = 85$ mmol/L, $\phi_{3\mathrm{MP}} = 0.09$, and $T = 281.8$ K. That is, the magnitude of f_{vdW} is sufficiently small compared with that of f_{ele}.

f_{Hel} arises from the entropic confinement of a fluctuating membrane by neighboring membranes.[45] In the case of the lamellar structure including an ionic surfactant, this effect can usually be neglected, since the electrostatic interaction between membranes suppresses the undulation.[23,33] Similarly, it should be reasonable to neglect the effect of f_{Hel} for the ordered-lamellar-structure in the present case. This idea is confirmed by the temperature dependence of d (see Fig. 5(a)): if the steric interaction between membranes is dominant, the opposite behavior, i.e., the increase in d with T, should be observed. Other evidence is provided by the magnitude of

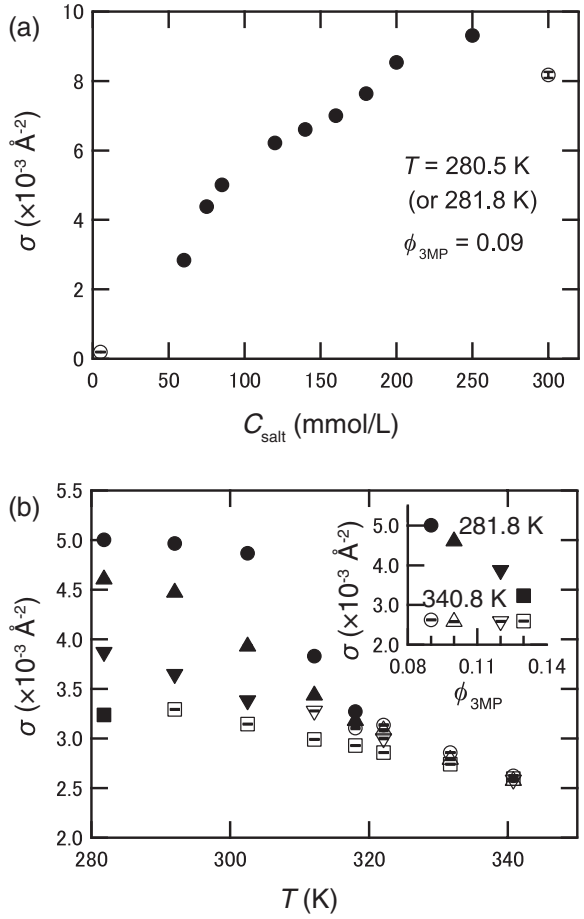

FIG. 11. The $C_{\rm salt}$, T, and $\phi_{\rm 3MP}$ dependences of σ according to Eq. (20) for the mixture of D_2O/3MP/$NaBPh_4$ both in the disordered-phase (open symbols) and the ordered-lamellar-phase (closed symbols). Error bars indicate ±1 standard deviation. (a) The $C_{\rm salt}$ dependence of σ at $\phi_{\rm 3MP} = 0.09$, and T is around 281 K. (b) The T dependence of σ at $C_{\rm salt} = 85$ mmol/L, $\phi_{\rm 3MP} = 0.09$, 0.10, 0.12, and 0.13. The inset shows the $\phi_{\rm 3MP}$ dependence of σ.

the Caillé parameter. If the steric interaction is dominant, the Caillé parameter $\eta_{\rm Hel}$ could be given by[33]

$$\eta_{\rm Hel} = \frac{4}{3}\left(1 - \frac{\delta}{d}\right)^2 \approx 1.0 \text{ to } 1.1. \tag{22}$$

This value is approximately twice as large as the present experimental results (see Fig. 3).

In this manner, it is interpreted that the electrostatic repulsion between membranes is the prime factor for stabilizing the long-range periodic structure in ordered-lamellar-phase. Additionally, it is pointed out that the "intramembrane interactions," i.e., the osmotic pressure arising from BPh_4^- ions in the 3MP-rich domains, $P_{\rm osm}$, or the dipole-dipole interaction arising from Na^+ and BPh_4^- ion pairs around the interface between D_2O-rich and 3MP-rich domains, $P_{\rm dipole}$, may also affect the morphology of the ordered-lamellar-structure. If we assume that $P_{\rm osm}$ and $P_{\rm dipole}$ result in decrease d, and their magnitudes increase with increasing $C_{\rm salt}$, the decrease of d above $C_{\rm salt} = 85$ mmol/L (see Fig. 3(a)) is explained. In future, the distributions of Na^+ and BPh_4^- ions in the mixture should be investigated experimentally to discuss the details of the effect of $P_{\rm osm}$ and $P_{\rm dipole}$.

Figure 11(a) shows the $C_{\rm salt}$ dependence of σ according to Eq. (20) for the mixture at $\phi_{\rm 3MP} = 0.09$ around $T = 281$ K. σ has a maximum around $C_{\rm salt} = 250$ mmol/L. This result suggests that the number of BPh_4^- ions in 3MP-rich domains is saturated at $C_{\rm salt} > 250$ mmol/L. The value of σ in the ordered-lamellar-phase spans the range between 2.5×10^{-3} Å^{-2} and 1.0×10^{-2} Å^{-2}, which is comparable with that of the surface density of surfactant molecules in typical surfactant membranes.[33]

Figure 11(b) shows the temperature dependence of σ at $C_{\rm salt} = 85$ mmol/L and $\phi_{\rm 3MP} = 0.09$, 0.10, 0.12, and 0.13. σ increases with decreasing temperature for all the samples. The inset of Fig. 11(b) exhibits the $\phi_{\rm 3MP}$ dependence of σ at two different temperatures: the open and closed symbols indicate the data for $T = 340.8$ K (disordered-phase) and $T = 281.8$ K (ordered-lamellar-phase), respectively. At $T = 340.8$ K, σ is almost independent of $\phi_{\rm 3MP}$ with a value of about $\sigma = 2.6 \times 10^{-3}$ Å^{-2}. On the other hand, σ increases with decreasing $\phi_{\rm 3MP}$ at $T = 281.8$ K.

V. CONCLUSION

In the present study, we investigated the structural properties of the disordered-phase and ordered-lamellar-phase in the mixture of D_2O/3-methylpyridine (3MP)/$NaBPh_4$. The SANS results for the ordered-lamellar-phase were well explained by the product of the structure factor $S(Q)$ of the lamellar structure and the form factor $P(Q)$ of the planar membrane. The fit parameter, the difference in scattering length density distribution between membrane and bulk water $\Delta\rho$, is almost constant at 4.9×10^{10} cm^{-2}: this corresponds to the difference in the scattering length densities of D_2O ($\rho_{\rm D_2O} = 6.4 \times 10^{10}$ cm^{-2}) and 3MP ($\rho_{\rm 3MP} = 1.4 \times 10^{10}$ cm^{-2}). These results indicate that 3MP-rich domains behave as membranes in the bulk water, D_2O. The intermediate scattering functions measured using NSE supported the description of membrane structure for both the disordered-phase and the ordered-lamellar-phase: this is well explained by the stretched exponential function with the stretching exponent $\beta = 2/3$, and the decay rate is proportional to the cube of momentum transfer.

On the basis of the SANS and NSE results, we showed that the 3MP-rich domains are stretched as a membrane owing to the solvation effects of Na^+ and BPh_4^-, and the periodicity of the ordered-lamellar-structure is stabilized mainly by the effects of the electrostatic interactions between neighboring membranes.

ACKNOWLEDGMENTS

The authors thank Dr. Butler at the National Institute of Standards and Technology (NIST) for generous assistance with the experimental setup, and are indebted to Dr. Neumann at NIST, Professor Onuki at Kyoto University, and Dr. Fujii at The University of Tokyo for valuable discussions. They also acknowledge the helpful comments of the anonymous referees. The SANS and NSE experiments were performed

under the approval of the National Institute of Standards and Technology, U.S. Department of Commerce (Proposal No. 13549 for NG3-30m SANS instruments, 13157 and 14715 for NG7-30m SANS instruments, and 13952 for NG5-NSE spectrometer). The NSE experiment at iNSE was performed under the approval of the Institute for Solid State Physics, The University of Tokyo, at Japan Atomic Energy Agency, Tokai, Japan (Proposal No. 9617). This work was supported by Grant-in-Aid for Creative Scientific Research and Grant-in-Aid for Scientific Research on Priority Area "Soft Matter Physics" from the Ministry of Education, Culture, Sports, Science and Technology (MEXT) of Japan, Grant-in-Aid for the Global COE Program "The Next Generation of Physics, Spun from Universality and Emergence" by MEXT of Japan, and Grant-in-Aid for Atomic Energy Initiative Project by MEXT of Japan. H.S. was supported by Grant-in-Aid for Scientific Research A (Grant No. 23244088). K.S. was supported by Grant-in-Aid for Young Scientists B (Grant No. 23750031), and Sasakawa Scientific Research Grant from The Japan Science Society (Grant No. 23-320). This work utilized facilities supported in part by the National Science Foundation under Agreement No. DMR-0944772.

Certain trade names and company products have been identified in order to clarify the experimental procedure adequately. In no case does such identification imply recommendation or endorsement by the National Institute of Standards and Technology, nor does it imply that the products are necessarily the best for the purposes used.

[1] A. Onuki, *Phase Transition Dynamics* (Cambridge University Press, Cambridge, 2002).
[2] B. J. Hales, G. L. Bertrand, and L. G. Hepler, J. Phys. Chem. **70**, 3970 (1966).
[3] T. Takamuku, A. Yamaguchi, D. Matsuo, M. Tabata, M. Kumamoto, J. Nishimoto, K. Yoshida, T. Yamaguchi, M. Nagao, T. Otomo, and T. Adachi, J. Phys. Chem. B **105**, 6236 (2001).
[4] M. Misawa, K. Yoshida, K. Maruyama, H. Munemura, and Y. Hosokawa, J. Phys. Chem. Solids **60**, 1301 (1999).
[5] V. Balevicius and H. Fuess, Phys. Chem. Chem. Phys. **1**, 1507 (1999).
[6] A. Onuki, Phys. Rev. E **73**, 021506 (2006).
[7] S. A. Safran, *Statistical Thermodynamics of Surfaces, Interfaces, and Membranes* (Westview Press, 1994).
[8] K. Sadakane, H. Seto, H. Endo, and M. Shibayama, J. Phys. Soc. Jpn. **76**, 113602 (2007).
[9] K. Sadakane, A. Onuki, K. Nishida, S. Koizumi, and H. Seto, Phys. Rev. Lett. **103**, 167803 (2009).
[10] K. Sadakane, N. Iguchi, M. Nagao, H. Endo, Y. B. Melnichenko, and H. Seto, Soft Matter **7**, 1334 (2011).
[11] Strong light scattering is observed in the ordered-lamellar-phase due to the existence of μm-sized structure. Note that similar light scattering is also observed in the mixture for $0 < \phi_{3MP} \leq 0.04$ below 318 K, even though the ordered-lamellar-structure is not confirmed by SANS. The detailed structure in these conditions should be clarified in future studies.
[12] A. Onuki and H. Kitamura, J. Chem. Phys. **121**, 3143 (2004).
[13] A. Onuki, J. Chem. Phys. **128**, 224704 (2008).
[14] M. M. Muir, L. B. Zinner, L. A. Paguaga, and L. M. Torres, Inorg. Chem. **21**, 3448 (1982).
[15] C. J. Glinka, J. G. Barker, B. Hammouda, S. Krueger, J. J. Moyer, and W. J. Orts, J. Appl. Crystallogr. **31**, 430 (1998).
[16] S. R. Kline, J. Appl. Crystallogr. **39**, 895 (2006).
[17] M. Monkenbusch, R. Schatzler, and D. Richter, Nucl. Instrum. Methods A **399**, 301 (1997).
[18] M. Nagao, N. L. Yamada, Y. Kawabata, H. Seto, H. Yoshizawa, and T. Takeda, Physica B **385-386**, 1118 (2006).
[19] R. T. Azuah, L. R. Kneller, Y. Qiu, P. L. W. Tregenna-Piggott, C. M. Brown, J. R. D. Copley, and R. M. Dimeo, J. Res. Natl. Inst. Stand. Technol. **114**, 341 (2009).
[20] L. S. Ornstein and F. Zernike, Proc. Akad. Wet. Amsterdam **17**, 793 (1914).
[21] H. E. Stanley, *Introduction to Phase Transitions and Critical Phenomena* (Oxford University Press, Oxford, 1971).
[22] According to our microscopic observation in D_2O/3MP/$NaBPh_4$ at $\phi_{3MP} = 0.09$ and $T = 283.2$ K, the ordered-lamellar-phase was not confirmed when $C_{salt} \leq 50$ mmol/L.
[23] J. N. Israelachvili, *Intermolecular and Surface Forces* (Academic Press, London, 1991).
[24] D. Roux, C. Coulon, and M. E. Cates, J. Phys. Chem. **96**, 4174 (1992).
[25] N. Lei, C. R. Safinya, D. Roux, and K. S. Liang, Phys. Rev. E **56**, 608 (1997).
[26] P. Lindner and T. Zemb, *Neutron, X-Rays and Light: Scattering Methods Applied to Soft Condensed Matter* (North Holland, 2002).
[27] L. Porcar, W. A. Hamilton, P. D. Butler, and G. G. Warr, Langmuir **19**, 10779 (2003).
[28] F. Nallet, R. Laversanne, and D. Roux, J. Phys. II **3**, 487 (1993).
[29] Y. Suganuma, N. Urakami, R. Mawatari, S. Komura, K. Nakaya-Yaegashi, and M. Imai, J. Chem. Phys. **129**, 134903 (2008).
[30] K. Minewaki, T. Kato, H. Yoshida, M. Imai, and K. Ito, Langmuir **17**, 1864 (2001).
[31] A. Caille, C. R. Acad. Sci. Ser. B **274**, 891 (1972).
[32] Y. Marcus, *Ion Solvation* (Wiley, 1985).
[33] D. Roux and C. R. Safinya, J. Phys. **49**, 307 (1988).
[34] R. Oda and J. D. Litster, J. Phys. II **7**, 815 (1997).
[35] F. Brochard and J. F. Lennon, J. Phys. **36**, 1035 (1975).
[36] R. B. Tishler and F. D. Carlson, Biophys. J. **51**, 993 (1987).
[37] E. Frey and D. R. Nelson, J. Phys. I **1**, 1715 (1991).
[38] B. Farago, M. Monkenbusch, K. D. Goecking, D. Richter, and J. S. Huang, Physica B **213-214**, 712 (1995).
[39] A. G. Zilman and R. Granek, Phys. Rev. Lett. **77**, 4788 (1996).
[40] E. Freyssingeas and D. Roux, J. Phys. II **7**, 913 (1997).
[41] T. Takeda, Y. Kawabata, H. Seto, S. Komura, S. K. Ghosh, M. Nagao, and D. Okuhara, J. Phys. Chem. Solids **60**, 1375 (1999).
[42] I. Javierre, F. Nallet, A. M. Bellocq, and M. Maugey, J. Phys.: Condens. Matter **12**, A295 (2000).
[43] T. Schilling, O. Theissen, and G. Gompper, Eur. Phys. J. E **4**, 103 (2001).
[44] E. Freyssingeas, A. Martin, and D. Roux, Eur. Phys. J. E **18**, 219 (2005).
[45] W. Helfrich, Z. Naturforsch. C **28**, 693 (1973).
[46] C. H. Cho, J. Urquidi, S. Singh, and G. W. Robinson, J. Phys. Chem. B **103**, 1991 (1999).
[47] Z. Yi, M. Nagao, and D. P. Bossev, J. Phys.: Condens. Matter **21**, 155104 (2009).
[48] M. Nagao, Phys. Rev. E **80**, 031606 (2009).
[49] M. C. Watson and F. L. H. Brown, Biophys. J. **98**, L9 (2010).
[50] J.-H. Lee, S.-M. Choi, C. Doe, A. Faraone, P. A. Pincus, and S. R. Kline, Phys. Rev. Lett. **105**, 038101 (2010).
[51] E. R. Nightingale, J. Phys. Chem. **63**, 1381 (1959).
[52] L. Porcar, J. Marignan, C. Ligoure, and T. Gulik-Krzywicki, Langmuir **16**, 2581 (2000).
[53] S. Leikin, V. A. Parsegian, D. C. Rau, and R. P. Rand, Annu. Rev. Phys. Chem. **44**, 369 (1993).